Evidence That Hepatic Lipase and Endothelial Lipase Have Different Substrate Specificities for High-Density Lipoprotein Phospholipids†

MyNgan Duong,[‡,§,||] Maria Psaltis,[§] Daniel J. Rader,[⊥] Dawn Marchadier,[⊥] Philip J. Barter,[‡,§,#] and Kerry-Anne Rye*[,§,#]

Department of Medicine, University of Adelaide, North Terrace, and Lipid Research Laboratory, Hanson Institute, Adelaide, South Australia, Australia 5000, and Department of Medicine, University of Pennsylvania School of Medicine, Philadelphia, Pennsylvania 19104

Received June 10, 2003; Revised Manuscript Received August 28, 2003

ABSTRACT: Hepatic lipase (HL) and endothelial lipase (EL) are both members of the triglyceride lipase gene family. HL hydrolyzes phospholipids and triglycerides in triglyceride-rich lipoproteins and high-density lipoproteins (HDL). EL hydrolyzes HDL phospholipids and has low triglyceride lipase activity. The aim of this study was to determine if HL and EL hydrolyze different HDL phospholipids and whether HDL phospholipid composition regulates the interaction of EL and HL with the particle surface. Spherical, reconstituted HDL (rHDL) containing either 1-palmitoyl-2-oleoylphosphatidylcholine (POPC), 1-palmitoyl-2-linoleoylphosphatidylcholine (PLPC), 1-palmitoyl-2-arachidonylphosphatidylcholine (PAPC), or 1-palmitoyl-2-docosahexanoylphosphatidylcholine (PDPC) as the only phospholipid, apolipoprotein A-I as the only apolipoprotein, and either cholesteryl esters (CE) only or mixtures of CE and triolein (TO) in their core were prepared. The rHDL were similar in size and had comparable core lipid/apoA-I molar ratios. The CE-containing rHDL were used to determine the kinetics of HL- and EL-mediated phospholipid hydrolysis. For HL the V_{max} of phospholipid hydrolysis for (POPC)rHDL > (PLPC)rHDL ∼ (PDPC)rHDL > (PAPC)rHDL, while the K_m(app) for (POPC)rHDL > (PDPC)rHDL > (PLPC)rHDL > (PAPC)rHDL. For EL the V_{max} for (PDPC)rHDL > (PAPC)rHDL > (PLPC)rHDL ∼ (POPC)rHDL, while the K_m(app) for (PAPC)rHDL ∼ (PLPC)rHDL > (POPC)rHDL > (PDPC)rHDL. The kinetics of EL- and HL-mediated TO hydrolysis was determined using rHDL that contained TO in their core. For HL the V_{max} of TO hydrolysis for (PLPC)rHDL > (POPC)rHDL > (PAPC)rHDL > (PDPC)rHDL, while the K_m(app) for (PLPC)rHDL > (POPC)rHDL ∼ (PAPC)rHDL > (PDPC)rHDL. For EL the V_{max} and K_m(app) for (PAPC)rHDL > (PDPC)rHDL > (PLPC)rHDL > (POPC)rHDL. These results establish that EL and HL have different substrate specificities for rHDL phospholipids and that their interactions with the rHDL surface are regulated by phospholipids.

The triglyceride lipase gene family consists of several members that have phospholipase and/or triglyceride lipase activities. Three members of this family, hepatic lipase (HL),[1] endothelial lipase (EL), and lipoprotein lipase (LPL) play key roles in lipoprotein metabolism. EL shares 45% homology with LPL and 40% homology with HL (*1*). HL and LPL hydrolyze the phospholipids and triglycerides in triglyceride-rich lipoproteins and high-density lipoproteins (HDL) (*2*). EL, by contrast, has low, but detectable, triglyceride lipase activity and preferentially hydrolyzes HDL phospholipids (*1*, *3*).

The enzymes vary widely in their tissue distribution. LPL is expressed by adipocytes, as well as cardiac and skeletal myocytes (*4*), while HL is expressed by hepatocytes (*5*). HL mRNA has also been detected in macrophages (*6*). EL is expressed by a wide range of tissues including hepatocytes, macrophages, and, uniquely within this family, endothelial cells (*1*, *7*).

Overexpression of EL in mice decreases HDL levels (*8*, *9*). This observation has been attributed to the high phospholipase activity of EL (*8*). More recent studies showing that HDL levels are raised in EL knockout mice (*9*), and that the activity of EL can be inhibited with polyclonal antibodies, strengthen the notion that this enzyme regulates HDL levels. Studies of HL knockout mice, which have elevated HDL levels (*10*), and mice transgenic for HL, which

† This work was supported by the National Health and Medical Research Council of Australia (Grant 200501) and a Pfizer International HDL Research Award. K.-A.R. is a Principal Research Fellow of the National Heart Foundation of Australia. M.D. was supported by a Helpman Scholarship in Cardiovascular Research.

* Address correspondence to this author at The Heart Research Institute. Telephone: +61-2-9550-3560. Fax: +61-2-9550-3302. E-mail: karye@ozemail.com.au or k.rye@hri.org.au.

‡ University of Adelaide.

§ Hanson Institute.

|| Current address: Joseph Stokes, Jr., Research Institute, Children's Hospital of Philadelphia, Philadelphia, PA 19104-4318.

⊥ University of Pennsylvania School of Medicine.

Current address: The Heart Research Institute, 145 Missenden Road, Camperdown, Sydney, New South Wales, Australia 2050.

[1] Abbreviations: apoA-I, apolipoprotein A-I; BHT, butylated hydroxytoluene; CE, cholesteryl esters; CETP, cholesteryl ester transfer protein; EL, endothelial lipase; LCAT, lecithin:cholesterol acyltransferase; LPL, lipoprotein lipase; HDL, high-density lipoprotein(s); HL, hepatic lipase; NEFA, nonesterified fatty acid(s); PAPC, 1-palmitoyl-2-arachidonylphosphatidylcholine; PDPC, 1-palmitoyl-2-docosahexanoylphosphatidylcholine; PLPC, 1-palmitoyl-2-linoleoylphosphatidylcholine; POPC, 1-palmitoyl-2-oleoylphosphatidylcholine; rHDL, reconstituted HDL; TBS, Tris-buffered saline; TO, triolein; UC, unesterified cholesterol.

10.1021/bi034990n CCC: $25.00
Published on Web 11/01/2003

have very low HDL levels (*11*), suggest that this may also be the case for HL.

These findings raise the question as to whether the phospholipase activities of HL and EL decrease levels of the same or different HDL subpopulations. This is an issue of considerable importance given that the HDL phospholipids in human plasma vary according to diet (*12*) and as a consequence of interactions with plasma factors such as phospholipid transfer protein and cholesteryl ester transfer protein (CETP) (*13*, *14*).

Phosphatidylcholine is the most abundant HDL phospholipid (*15*). HDL phosphatidylcholine *sn*-2 acyl chains vary in length and unsaturation, with 1-palmitoyl-2-oleoylphosphatidylcholine (POPC), 1-palmitoyl-2-linoleoylphosphatidylcholine (PLPC), 1-palmitoyl-2-arachidonylphosphatidylcholine (PAPC), and 1-palmitoyl-2-docosahexanoylphosphatidylcholine (PDPC), respectively, comprising 12.9%, 34.4%, 9.1%, and 3.6% of the total HDL phosphatidylcholine (*16*).

To determine if EL and HL hydrolyze these phospholipids equally well, it is important to use HDL in which the phospholipid composition varies systematically but which are comparable in size, apolipoprotein content, and core lipid/apolipoprotein molar ratio. The HDL in human plasma are inappropriate for studies of this type because they consist of mixtures of particles that vary widely in their phospholipid and apolipoprotein content (*17*, *18*). There is also considerable variation in the size and core lipid/apolipoprotein molar ratio of human HDL (*17*).

These problems have been circumvented in the present study by using well-characterized preparations of spherical reconstituted HDL (rHDL) that are comparable in size, have similar core lipid/apolipoprotein molar ratios, contain either POPC, PLPC, PAPC, or PDPC as the only phospholipid, and contain apolipoprotein A-I (apoA-I) as the only apolipoprotein (*19*). These preparations were used to study the kinetics of EL- and HL-mediated phospholipid hydrolysis. The results show clearly that HL and EL preferentially hydrolyze different phospholipids in spherical rHDL and that phospholipids regulate the interaction of EL and HL with the rHDL surface.

EXPERIMENTAL PROCEDURES

Isolation of ApoA-I. HDL were isolated by sequential ultracentrifugation ($1.07 < d < 1.21$ g/mL) from pooled, autologously donated human plasma samples (Gribbles Pathology, Adelaide, Australia). The HDL were delipidated using solvent extraction (*20*). ApoA-I was isolated from the resulting apoHDL by chromatography on a Q-Sepharose Fast-Flow column (Amersham Biosciences) attached to a fast protein liquid chromatography system (Amersham Biosciences) (*21*, *22*). The isolated apoA-1 appeared as a single band when subjected to electrophoresis on a homogeneous 20% SDS−polyacrylamide PhastGel (Amersham Biosciences) and Coomassie staining.

Isolation of Lecithin:Cholesterol Acyltransferase (LCAT). LCAT was isolated from pooled samples of human plasma by protein precipitation, ultracentrifugation, hydrophobic interaction chromatography, and ion-exchange chromatography (*23*). LCAT activity was determined as described using 1-palmitoyl-2-oleoylphosphatidylcholine (POPC)/UC/apoA-I discoidal rHDL ^{3}H-labeled with unesterified cholesterol (UC) (Sigma) as the substrate (*24*). Cholesterol esterification was linear with respect to time as long as less than 30% of the [^{3}H]UC was esterified. The LCAT preparations used in this study generated 995−1590 nmol of cholesteryl esters (CE) (mL of LCAT)$^{-1}$ h^{-1}.

Isolation of Cholesteryl Ester Transfer Protein (CETP). CETP was isolated from pooled samples of human plasma by ammonium sulfate precipitation, ultracentrifugation, hydrophobic interaction chromatography, and ion-exchange chromatography (*25*). The activities of the preparations were assessed as the transfer of [^{3}H]CE from [^{3}H]CE-HDL$_3$ to low-density lipoproteins (*26*, *27*). The assay was linear with respect to time as long as less than 30% of the [^{3}H]CE was transferred. The activities of the CETP preparations used in this study varied from 22.7 to 48.2 units of activity/mL, where 1 unit is the transfer activity of 1 mL of a preparation of pooled, human lipoprotein-deficient plasma.

Preparation of Spherical rHDL. Discoidal rHDL containing either POPC, PLPC, PAPC, or PDPC (Sigma), UC, and apoA-I were prepared by the cholate dialysis method (*28*). The discoidal rHDL were converted into spherical rHDL by incubation with LCAT and UC as described (*19*). The resulting spherical rHDL were isolated by sequential ultracentrifugation in the $1.07 < d < 1.21$ g/mL density range and dialyzed against 0.01 mol/L Tris-buffered saline (TBS) (pH 7.4) containing 0.15 mol/L NaCl, 0.006% (w/v) NaN_3, 50 μmol/L diethylenetriaminepentaacetic acid (Sigma), and butylated hydroxytoluene (BHT) (final concentration 10 μmol/L) (Sigma). The spherical rHDL were stored under argon at 4 °C in the presence of Chelex 100 resin (Bio-Rad, Hercules, CA).

Preparation of Microemulsions. Microemulsions containing triolein (TO) and either POPC, PLPC, PAPC, or PDPC were prepared by sonication (*29*). The phospholipids (37.5 mg) and TO (100 mg) were dissolved in chloroform−methanol (2:1 v/v). BHT (final concentration 0.12 mmol/L) was added to inhibit inadvertent oxidation. The mixtures were dried under a stream of N_2 for 2 h and maintained overnight under vacuum. TBS (12 mL) was added to the lipids, and the resulting solutions were sonicated as described (*29*). The microemulsions were isolated by ultracentrifugation as the fraction of $d < 1.21$ g/mL.

Preparation of [^{3}H]TO-Labeled Spherical rHDL. [^{3}H]TO-labeled POPC/TO, PLPC/TO, PAPC/TO, and PDPC/TO microemulsions were prepared as described (*30*). Spherical rHDL were labeled with [^{3}H]TO (28 Ci/mmol) (NEN Life Science Products) by incubation at 37 °C under N_2 for 1−3 h with CETP and an appropriate [^{3}H]TO-labeled microemulsion. To ensure that the rHDL phospholipid composition did not change during the incubations, the (POPC)rHDL, (PLPC)rHDL, (PAPC)rHDL, and (PDPC)rHDL were respectively incubated with microemulsions containing either POPC, PLPC, PAPC, or PDPC as the only phospholipid. The resulting [^{3}H]TO-enriched rHDL were isolated by sequential ultracentrifugation in the $1.063 < d < 1.21$ g/mL density range. Enrichment with TO increased the diameter of the rHDL by up to 10%. The [^{3}H]TO−(POPC)rHDL, [^{3}H]TO−(PLPC)rHDL, [^{3}H]TO−(PAPC)rHDL, and [^{3}H]TO−(PDPC)rHDL were concentrated 7-, 4-, 4.5-, and 5-fold before use. Their respective specific activities were 9.9×10^6, 2.4×10^6, 1.6×10^6, and 4.3×10^6 cpm/mg TO.

Isolation of HL. HL was isolated from pooled samples of postheparin plasma. Fifty milliliters of blood was obtained

from each of 35 patients. The patients were injected with a bolus of 25000 IU of heparin prior to undergoing percutaneous transluminal coronary angioplasty (Cardiovascular Investigation Unit, Royal Adelaide Hospital). Postheparin plasma was isolated by centrifugation at 3000 rpm for 10 min at 4 °C and stored at −80 °C until use. HL was isolated from the thawed plasma by heparin−Sepharose Fast-Flow chromatography (Amersham Biosciences) (*30*). The activities of the HL preparations were determined by incubating mixtures of spherical (POPC)rHDL (20 nmol of phospholipid), BSA (final concentration of 20 mg/mL), and HL (25 μL) at 37 °C for 1 h. The final volume of the incubation mixtures was 140 μL. The nonesterified fatty acid (NEFA) mass was quantitated using a commercially available kit (Wako Pure Chemical Industries, Osaka, Japan). The HL preparations used in this study generated 32−122 nmol of NEFA (mL of HL)$^{-1}$ h^{-1}.

Expression of EL. COS cells were grown in Dulbecco's modified Eagle medium (DMEM) with 10% fetal bovine serum (FBS) and 1% antibiotic/antimyotic (A/A) at 37 °C and 5% CO_2. Prior to infection, cells were brought to 90% confluency in 150 mm plates. Growth medium was removed, and the cells were washed with 10 mL of serum-free DMEM without phenol red and then incubated with recombinant adenovirus encoding EL in 5 mL of the same medium at a multiplicity of 3000 particles/ cell. Two hours later, 9 mL of serum-free medium without phenol red, containing 10 units/mL heparin, was added to each of the plates. At 47.5 h postinfection, an additional 10 units/mL heparin (280 μL of 500 units/mL) was added, and cells were incubated for 30 min. Medium was collected and clarified by centrifugation at 2000 rpm for 10 min in 50 mL conical tubes and then frozen in 1 mL aliquots at −80 °C. A single preparation of EL that generated 600 nmol of NEFA (mL of EL)$^{-1}$ h^{-1} was used for this study. Activity was determined as described (*3*).

Kinetic Studies. All incubations were carried out under N_2 in stoppered tubes in a shaking water bath maintained at 37 °C. Varying concentrations of rHDL were mixed with BSA, TBS, and a constant amount of either HL or EL. Details of the individual incubations are described in the figure legends. When the incubations were complete, the tubes were placed immediately on ice.

Phospholipid hydrolysis was determined by quantitating the mass of NEFA formed, assuming that 1 mol of NEFA is produced for each mole of phospholipid hydrolyzed. TO hydrolysis was determined by adding 1 mL of chloroform−methanol (2:1 v/v) to the chilled incubation mixtures and extracting the lipids (*31*). NEFA and TO were separated by TLC (30), cut from the sheets, and counted using a Beckman LS 6000TA liquid scintillation counter (Beckman Instruments, Fullerton, CA).

The kinetic parameters, V_{max} and K_m(app), were derived by nonlinear regression analysis using GraphPad Prism version 4.02a for the Macintosh (GraphPad Software) and the equation $Y = V_{max}X/(K_m + X)$. As the HL- and EL-mediated phospholipid and TO hydrolysis occurred at an interface, and not in the presence of a monomeric substrate, "classical" kinetic parameters could not be derived. For this reason "apparent" K_m values are reported. In all cases significance was set at $p < 0.05$. The catalytic efficiency of the hydrolysis reaction is reported as V_{max}/K_m(app). There are numerous precedents in the literature for using this ratio as a measure of the efficiency of a two-step catalytic mechanism (*32*, *33*).

Table 1: Physical Properties of Spherical rHDL

spherical rHDL[a]	Stokes diameter (nm)[b]	stoichiometry (mol/mol)[c]				
		PL	UC	CE	TG	A-I
(POPC)rHDL	8.8	25.2	0.8	19.2	0.0	1.0
(PLPC)rHDL	9.0	34.5	1.5	21.6	0.0	1.0
(PAPC)rHDL	9.1	34.6	3.1	20.2	0.0	1.0
(PDPC)rHDL	9.2	25.8	2.2	17.0	0.0	1.0
[^{3}H]TO−(POPC)rHDL	9.5	51.7	0.9	19.4	5.8	1.0
[^{3}H]TO−(PLPC)rHDL	10.0	50.8	1.5	16.1	9.3	1.0
[^{3}H]TO−(PAPC)rHDL	9.8	53.1	0.9	16.8	7.2	1.0
[^{3}H]TO−(PDPC)rHDL	9.8	47.3	1.3	14.7	7.0	1.0

[a] Spherical rHDL were prepared by adding LCAT and unesterified cholesterol to discoidal rHDL as described under Experimental Procedures. The spherical rHDL were isolated by ultracentrifugation, and their composition was determined as described. TO-rHDL were prepared by incubating the rHDL (final concentration 0.1 mmol/L CE) with [^{3}H]TO-labeled microemulsions (final concentration 4.0 mmol/L TG) and CETP (final activity 2.7 units/mL). Final volumes of these incubations ranged from 23.9 mL for [^{3}H]TO−(PDPC)rHDL to 30.6 mL for [^{3}H]TO−(PLPC)rHDL. [b] Determined by nondenaturing gradient gel electrophoresis. [c] Abbreviations: PL, phospholipid; CE, cholesteryl ester; UC, unesterified cholesterol; A-1, apolipoprotein A-I; TG, triglycerides.

Other Techniques. An Hitachi 902 automatic analyzer (Roche Diagnostics, Mannheim, Germany) was used for all chemical analyses. Phospholipid concentrations were determined as described by Takayama et al. (*34*). Total cholesterol assays were carried out using a commercially available kit (Roche Diagnostics). Unesterified cholesterol was measured as described (*35*). CE concentrations were determined as the difference between UC and total cholesterol concentrations. TO concentrations were assayed as described (*36*). The bicinchoninic acid assay was used to quantitate apoA-I concentrations (*37*). Nondenaturing 3−35% gradient gel electrophoresis was used to determine rHDL particle size (*18*).

RESULTS

Physical Properties of Spherical (POPC)rHDL, (PLPC)rHDL, (PAPC)rHDL, and (PDPC)rHDL (Table 1). The (POPC)rHDL, (PLPC)rHDL, (PAPC)rHDL, and (PDPC)rHDL that contained CE as the only core lipid had comparable CE/apoA-I and phospholipid/apoA-1 molar ratios (Table 1). Each preparation consisted of a single, monodisperse population of particles with diameters ranging from 8.8 nm for the (POPC)rHDL to 9.2 nm for the (PDPC)rHDL.

Kinetics of HL-Mediated Phospholipid Hydrolysis in (POPC)rHDL, (PLPC)rHDL, (PAPC)rHDL, and (PDPC)rHDL (Figure 1, Table 2A). Varying concentrations of (POPC)rHDL (closed circles), (PLPC)rHDL (closed triangles), (PAPC)rHDL (open circles), and (PDPC)rHDL (open triangles) (100−1000 μmol/L phospholipid) were incubated at 37 °C for 1 h with a constant amount of HL. NEFA mass was measured directly. Nonlinear regression analysis of the rate of phospholipid hydrolysis as a function of rHDL phospholipid concentration is shown in Figure 1A. As judged by two-way Anova, the results for the (POPC)rHDL, (PLPC)rHDL, (PAPC)rHDL, and (PDPC)rHDL were all significantly different from each other ($p < 0.0001$). Lineweaver−Burk plots of the kinetic data are shown in Figure 1B.

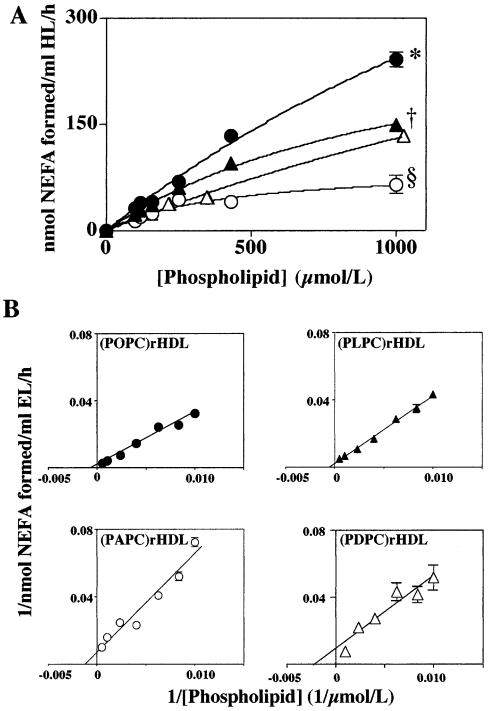

FIGURE 1: Hydrolysis of phospholipids in (POPC)rHDL, (PLPC)rHDL, (PAPC)rHDL, and (PDPC)rHDL by HL. Varying concentrations of (POPC)rHDL (●), (PLPC)rHDL (▲), (PAPC)rHDL (○), and (PDPC)rHDL (△) (100−1000 μmol/L phospholipid) were incubated at 37 °C for 3 h with BSA (final concentration 20 mg/mL) and a constant amount of HL [24 μL of a preparation that generated 32 nmol of NEFA (mL of HL)$^{-1}$ h^{-1}]. The final incubation volume was 120 μL. Panel A shows the line of best fit for the rate of HL-mediated phospholipid hydrolysis as a function of substrate concentration for each rHDL preparation (mean ± SEM of triplicate determinations). Lineweaver−Burk plots are shown in panel B. Key: *, $p < 0.0001$ for (POPC)rHDL versus (PLPC)rHDL, (POPC)rHDL versus (PAPC)rHDL, and (POPC)rHDL versus (PDPC)rHDL; †, $p < 0.0001$ for (PLPC)rHDL versus (PAPC)rHDL and (PLPC)rHDL versus (PDPC)rHDL; §, $p < 0.0001$ for (PAPC)rHDL versus (PDPC)rHDL.

Nonlinear regression analysis was used to derive the kinetic parameters. The values are expressed as the mean ± SEM (Table 2A). The V_{max} of phospholipid hydrolysis for (POPC)rHDL, (PLPC)rHDL, (PAPC)rHDL, and (PDPC)rHDL was 800.0 ± 42.5, 346.3 ± 12.9, 147.4 ± 20.4, and 365.1 ± 60.2 nmol of NEFA formed (mL of HL)$^{-1}$ h^{-1}, respectively. The respective K_m(app) for (PAPC)rHDL and (PDPC)rHDL was 936.0 ± 265.7 and 1993.0 ± 421.4 μmol/L phospholipid, compared to 1250.0 ± 87.9 and 2327.0 ± 195.3 μmol/L phospholipid for (PLPC)rHDL and (POPC)rHDL. The catalytic efficiencies [V_{max}/K_m(app)] for phospholipid hydrolysis ranged from 0.34 for (POPC)rHDL to 0.16 for (PAPC)rHDL.

Kinetics of EL-Mediated Phospholipid Hydrolysis in (POPC)rHDL, (PLPC)rHDL, (PAPC)rHDL, and (PDPC)rHDL (Figure 2, Table 2A). Varying amounts of (POPC)rHDL (closed circles), (PLPC)rHDL (closed triangles), (PAPC)rHDL (open circles), and (PDPC)rHDL (open triangles) (100−1000 μmol/L phospholipid) were incubated at 37 °C for 0.5 h with a constant amount of EL. NEFA mass was measured directly. Nonlinear regression analysis of the rate of phospholipid hydrolysis as a function of rHDL phospholipid concentration is shown in Figure 2A. As judged by two-way Anova, the kinetics of phospholipid hydrolysis was comparable for (POPC)rHDL and (PLPC)rHDL. The results for (POPC)rHDL versus (PAPC)rHDL were significantly different at the level of $p < 0.05$, compared to $p < 0.005$ for (PLPC)rHDL versus (PAPC)rHDL. The results for (POPC)rHDL versus (PDPC)rHDL and (PDPC)rHDL versus (PAPC)rHDL were also significantly different ($p < 0.0001$). Lineweaver−Burk plots of the kinetic data are shown in Figure 2B.

The V_{max} of phospholipid hydrolysis for (PDPC)rHDL and (PAPC)rHDL was 233.4 ± 25.3 and 184.0 ± 23.5 nmol of NEFA generated (mL of EL)$^{-1}$ h^{-1}, respectively, compared with 133.5 ± 12.4 and 146.3 ± 18.8 nmol of NEFA generated (mL of EL)$^{-1}$ h^{-1} for (POPC)rHDL and (PLPC)rHDL (Table 2A). The respective K_m(app) values for (POPC)rHDL, (PLPC)rHDL, (PAPC)rHDL, and (PDPC)rHDL were 208.7 ± 52.6, 294.9 ± 90.6, 274.2 ± 85.9, and 139.7 ± 44.3 μmol/L phospholipid. The catalytic efficiency of phospholipid hydrolysis was 2−3-fold greater for (PDPC)rHDL than for any of the other rHDL.

Physical Properties of [^{3}H]TO−(POPC)rHDL, [^{3}H]TO−(PLPC)rHDL, [^{3}H]TO−(PAPC)rHDL, and [^{3}H]TO−(PDPC)rHDL (Table 1). The [^{3}H]TO-enriched rHDL were larger than the original rHDL that contained only CE in their core. The diameters of the [^{3}H]TO-enriched rHDL ranged from 9.5 nm for [^{3}H]TO−(POPC)rHDL to 10.0 nm for [^{3}H]-TO−(PLPC)rHDL (Table 1). This is in agreement with what has been reported previously from this laboratory (*30*). The increase in the phospholipid/apoA-I molar ratios of the TO-enriched rHDL, relative to the rHDL that contained only CE in their core, reflects the spontaneous transfer of phospholipids from the microemulsions to the rHDL (*19*). The triglyceride/apoA-I molar ratio of the [^{3}H]TO−(POPC)rHDL was low compared to the other rHDL because of the reduced CETP-mediated transfer of TO from the POPC−TO microemulsions to the (POPC)rHDL. This is consistent with previous reports from this laboratory (*19*).

As the curvature of a sphere of radius R is $1/R^2$, it follows that the increase in rHDL size that occurred as a consequence of TO enrichment was associated with a reduction in the surface curvature of the particles. Previous reports from this laboratory have also established that spherical rHDL phospholipid headgroup and acyl chain packing order increases with increasing particle size (*25*). Although such changes in surface curvature and phospholipid packing order may influence hydrolysis rates, these effects are likely to be minor and have not been considered in the kinetic analysis.

Kinetics of HL-Mediated Triglyceride Hydrolysis in [^{3}H]-TO−(POPC)rHDL, [^{3}H]TO−(PLPC)rHDL, [^{3}H]TO−(PAPC)rHDL, and [^{3}H]TO−(PDPC)rHDL (Figure 3, Table 2B). In this study, [^{3}H]TO-enriched rHDL (50−350 μmol/L triglyceride) were incubated at 37 °C for 2 h with a constant amount of HL. Nonlinear regression analysis of the rate of HL-mediated TO hydrolysis in the [^{3}H]TO−(POPC)rHDL (closed circles), [^{3}H]TO−(PLPC)rHDL (closed triangles), [^{3}H]TO−(PAPC)rHDL (open circles), and [^{3}H]TO−(PDPC)-rHDL (open triangles) is shown in Figure 3A. All of the curves were significantly different from each other at the level of $p < 0.0001$ except for (POPC)rHDL versus (PLPC)-rHDL, where $p = 0.0011$. Lineweaver−Burk plots of the kinetic data are shown in Figure 3B.

The V_{max} of TO hydrolysis in (PDPC)rHDL and (PAPC)rHDL was 736.0 ± 145.6 and 1133.0 ± 188.8 nmol

Table 2: Kinetic Parameters for HL- and EL-Mediated Phospholipid Hydrolysis in Spherical (POPC)rHDL, (PLPC)rHDL, (PAPC)rHDL, and (PDPC)rHDL and for HL- and EL-Mediated Triglyceride Hydrolysis in Spherical [^{3}H]TO−(POPC)rHDL, [^{3}H]TO−(PLPC)rHDL, [^{3}H]TO−(PAPC)rHDL, and [^{3}H]TO−(PDPC)rHDL[a]

spherical rHDL	enzyme	constituent hydrolyzed	V_{max} [nmol of NEFA (mL of HL)$^{-1}$ h^{-1}]	K_m(app) (μmol/L PL)	catalytic efficiency V_{max}/K_m(app)
(A) HL- and EL-Mediated Phospholipid Hydrolysis in Spherical (POPC)rHDL, (PLPC)rHDL, (PAPC)rHDL, and (PDPC)rHDL					
(POPC)rHDL	HL	phospholipid	800.0 ± 42.5	2327.0 ± 195.3	0.34
(PLPC)rHDL	HL	phospholipid	346.3 ± 12.9	1250.0 ± 87.9	0.28
(PAPC)rHDL	HL	phospholipid	147.4 ± 20.4	936.0 ± 265.7	0.16
(PDPC)rHDL	HL	phospholipid	365.1 ± 60.21	1993.0 ± 421.4	0.18
(POPC)rHDL	EL	phospholipid	133.5 ± 12.4	208.7 ± 52.6	0.64
(PLPC)rHDL	EL	phospholipid	146.3 ± 18.8	294.9 ± 90.6	0.50
(PAPC)rHDL	EL	phospholipid	184.0 ± 23.5	274.2 ± 85.9	0.67
(PDPC)rHDL	EL	phospholipid	233.4 ± 25.3	139.7 ± 44.3	1.67
(B) HL- and EL-Mediated Triglyceride Hydrolysis in Spherical [^{3}H]TO−(POPC)rHDL, [^{3}H]TO−(PLPC)rHDL, [^{3}H]TO−(PAPC)rHDL, and [^{3}H]TO−(PDPC)rHDL					
[^{3}H]TO−(POPC)rHDL	HL	triglyceride	1270.0 ± 141.1	470.7 ± 78.0	2.70
[^{3}H]TO−(PLPC)rHDL	HL	triglyceride	1777.0 ± 148.1	677.8 ± 77.2	2.62
[^{3}H]TO−(PAPC)rHDL	HL	triglyceride	1133.0 ± 188.8	533.1 ± 125.8	2.12
[^{3}H]TO−(PDPC)rHDL	HL	triglyceride	736.1 ± 145.6	199.9 ± 78.2	3.68
[^{3}H]TO−(POPC)rHDL	EL	triglyceride	6.2 ± 0.3	8.1 ± 1.1	0.77
[^{3}H]TO−(PLPC)rHDL	EL	triglyceride	9.7 ± 0.3	6.6 ± 0.6	1.47
[^{3}H]TO−(PAPC)rHDL	EL	triglyceride	41.4 ± 1.9	47.2 ± 3.3	0.88
[^{3}H]TO−(PDPC)rHDL	EL	triglyceride	21.9 ± 1.0	22.9 ± 2.0	0.96

[a] Spherical rHDL were prepared as described under Experimental Procedures. Kinetic parameters were derived by a nonlinear regression analysis of the rate of phospholipid or TO hydrolysis versus the concentration of substrate.

of NEFA generated (mL of EL)$^{-1}$ h^{-1}, respectively, compared with 1270.0 ±141.1 and 1777.0 ± 148.1 nmol of NEFA generated (mL of EL)$^{-1}$ h^{-1} for (POPC)rHDL and (PLPC)rHDL (Table 2B). The respective K_m(app) values for (POPC)rHDL, (PLPC)rHDL, (PAPC)rHDL and (PDPC)rHDL were 470.7 ± 8.0, 677.8 ± 77.2, 533.1 ± 125.8, and 199.9 ± 78.2 μmol/L phospholipid. HL hydrolyzed the TO in (PDPC)rHDL more efficiently than the TO in the other rHDL.

Kinetics of EL-Mediated Triglyceride Hydrolysis in [^{3}H]-TO−(POPC)rHDL, [^{3}H]TO−(PLPC)rHDL, [^{3}H]TO−(PAPC)rHDL, and [^{3}H]TO−(PDPC)rHDL (Figure 4, Table 2B). For this study [^{3}H]TO−(POPC)rHDL (closed circles), [^{3}H]TO−(PLPC)rHDL (closed triangles), [^{3}H]TO−(PAPC)rHDL (open circles), and [^{3}H]TO−(PDPC)rHDL (open triangles) (6−40 μmol/L triglyceride) were incubated at 37 °C for 1 h with a constant amount of EL. In all cases, the rate of EL-mediated triglyceride hydrolysis was much less than what was observed for HL-mediated TO hydrolysis (Figure 3A). Nonlinear regression analysis of the rate of TO hydrolysis as a function of rHDL TO concentration is shown in Figure 4A. As judged by two-way Anova, the results for (POPC)rHDL, (PLPC)rHDL, (PAPC)rHDL, and (PDPC)rHDL were all significantly different from each other ($p < 0.0001$). Lineweaver−Burk plots of the kinetic data are shown in Figure 4B.

The V_{max} of TO hydrolysis in (PDPC)rHDL and (PAPC)rHDL was 21.9 ± 1.0 and 41.4 ± 1.9 nmol of NEFA generated (mL of EL)$^{-1}$ h^{-1}, respectively, compared with 6.2 ± 0.3 and 9.7 ± 0.3 nmol of NEFA generated (mL of EL)$^{-1}$ h^{-1} for (POPC)rHDL and (PLPC)rHDL (Table 2B). The respective K_m(app) values for (POPC)rHDL, (PLPC)rHDL, (PAPC)rHDL, and (PDPC)rHDL were 8.1 ± 1.1, 6.6 ± 0.6, 47.2 ± 3.3, and 22.9 ± 2.0 μmol/L TO. The catalytic efficiency of EL-mediated TO hydrolysis ranged from 0.77 for [^{3}H]TO−(POPC)rHDL to 1.47 for [^{3}H]TO−(PLPC)rHDL.

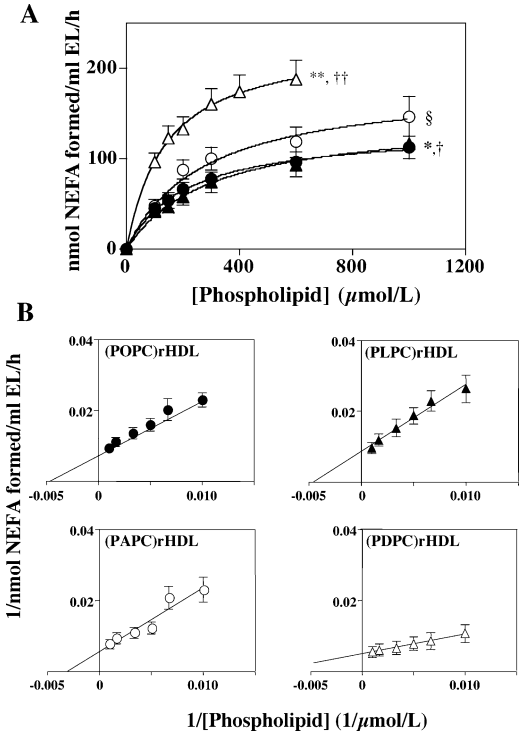

FIGURE 2: Hydrolysis of phospholipids in (POPC)rHDL, (PLPC)rHDL, (PAPC)rHDL, and (PDPC)rHDL by EL. Varying concentrations of (POPC)rHDL (●), (PLPC)rHDL (▲), (PAPC)rHDL (○), and (PDPC)rHDL (△) (100−1000 μmol/L phospholipid) were incubated at 37 °C for 0.5 h with BSA (final concentration 20 mg/mL) and a constant amount of EL [125 μL of a preparation that generated 60 nmol (mL of EL)$^{-1}$ h^{-1}]. The final incubation volume was 250 μL. Panel A shows the line of best fit for each rHDL preparation (mean ± SEM of triplicate determinations). Lineweaver−Burk plots are shown in panel B. Key: *, $p < 0.05$ for (POPC)rHDL versus (PAPC)rHDL; **, $p < 0.0001$ for (POPC)rHDL versus (PDPC)rHDL; †, $p < 0.005$ for (PLPC)rHDL versus (PAPC)rHDL; ††, $p < 0.0001$ for (PLPC)rHDL versus (PDPC)rHDL; §, $p < 0.0001$ for (PAPC)rHDL versus (PDPC)rHDL.

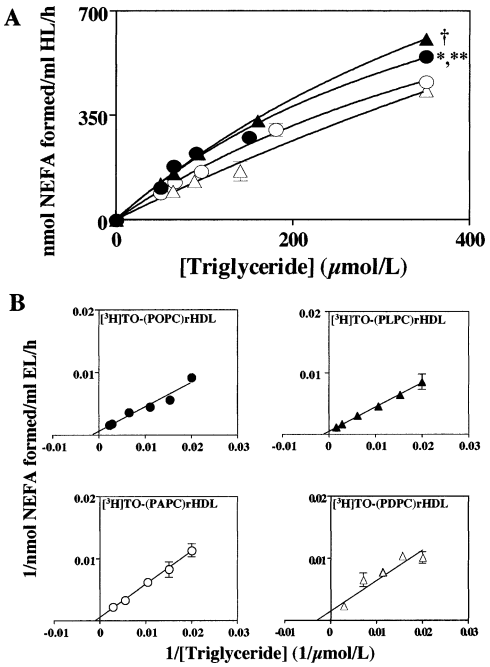

FIGURE 3: Hydrolysis of triolein in [^{3}H]TO−(POPC)rHDL, [^{3}H]-TO−(PLPC)rHDL, [^{3}H]TO−(PAPC)rHDL, and [^{3}H]TO−(PDPC)rHDL by HL. Varying concentrations of [^{3}H]TO−(POPC)rHDL (●), [^{3}H]TO−(PLPC)rHDL (▲), [^{3}H]TO−(PAPC)rHDL (○), and [^{3}H]TO−(PDPC)rHDL (△) (50−350 μmol/L triglyceride) were incubated at 37 °C for 2 h with BSA (final concentration 20 mg/mL) and a constant amount of HL [5 μL of a preparation that generated 122 nmol of NEFA (mL of HL)$^{-1}$ h^{-1}]. The final incubation volume was 50 μL. Panel A shows the line of best fit for each rHDL preparation (mean ± SEM of triplicate determinations). Lineweaver−Burk plots are shown in panel B. Key: *, $p = 0.0011$ for (POPC)rHDL versus (PLPC)rHDL; **, $p < 0.0001$ for (POPC)rHDL versus (PAPC)rHDL and (POPC)rHDL versus (PDPC)rHDL; †, $p < 0.0001$ for (PLPC)rHDL versus (PAPC)rHDL and (PLPC)rHDL versus (PDPC)rHDL.

Comparison of rHDL Phospholipid and TO Hydrolysis by HL and EL (Figure 5). To compare the abilities of EL and HL to hydrolyze TO and the different rHDL phospholipids directly, the kinetic parameters from the above experiments were normalized by adjusting the values for (POPC)rHDL (filled bars) to 100. The values for (PLPC)rHDL (open bars), (PAPC)rHDL (vertical bars), and (PDPC)rHDL (diagonal bars) are expressed relative to (POPC)rHDL (Figure 5).

For HL-mediated phospholipid hydrolysis the values for the V_{max} and K_m(app) were higher for (POPC)rHDL than for any of the other rHDL. HL also hydrolyzed the phospholipids in (POPC)rHDL and (PLPC)rHDL more efficiently than the phospholipids in (PAPC)rHDL and (PDPC)rHDL. For HL-mediated TO hydrolysis the values for the V_{max} and K_m(app) for (PLPC) were higher than for the other rHDL. HL hydrolyzed the TO in (PDPC)rHDL more efficiently than in the other rHDL. This was a reflection of the high affinity [lower K_m(app)] of HL for the TO in (PDPC)rHDL.

EL hydrolyzed the phospholipids in (PDPC)rHDL approximately 3-fold more efficiently than the phospholipids in any of the other rHDL. This was a reflection of the higher V_{max} and lower K_m(app) of EL for (PDPC)rHDL than for any of the other rHDL. The catalytic efficiency of EL-mediated TO hydrolysis in (PLPC)rHDL was approximately double that of the other rHDL.

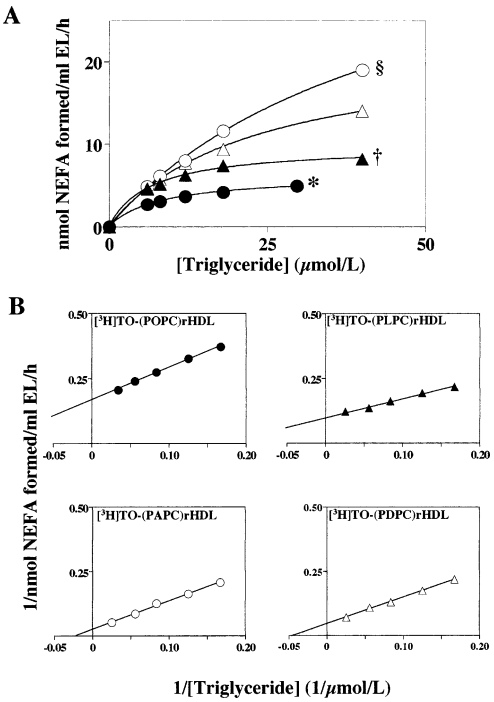

FIGURE 4: Hydrolysis of triolein in [^{3}H]TO−(POPC)rHDL, [^{3}H]-TO−(PLPC)rHDL, [^{3}H]TO−(PAPC)rHDL, and [^{3}H]TO−(PDPC)rHDL by EL. Varying concentrations of [^{3}H]TO−(POPC)rHDL (●), [^{3}H]TO−(PLPC)rHDL (▲), [^{3}H]TO−(PAPC)rHDL (○), and [^{3}H]TO−(PDPC)rHDL (△) (6−40 μmol/L triglyceride) were incubated at 37 °C for 1 h with BSA (final concentration 20 mg/mL) and a constant amount of EL [20 μL of a preparation that generated 50 nmol of NEFA (mL of EL)$^{-1}$ h^{-1}]. The final incubation volume was 50 μL. Panel A shows the line of best fit for each rHDL preparation (mean ± SEM of triplicate determinations). The corresponding Lineweaver−Burk plots are shown in panel B. Key: *, $p < 0.0001$ for (POPC)rHDL versus (PLPC)rHDL, (POPC)rHDL versus (PAPC)rHDL, and (POPC)rHDL versus (PDPC)rHDL; †, $p < 0.0001$ for (PLPC)rHDL versus (PAPC)rHDL and (PLPC)rHDL versus (PDPC)rHDL; §, $p < 0.0001$ for (PAPC)rHDL versus (PDPC)rHDL.

DISCUSSION

HL and EL are both members of the triglyceride lipase gene family that have substantial phospholipase activity but differ widely in their ability to hydrolyze HDL triglycerides. While HL hydrolyzes HDL triglycerides effectively (*2*), EL has very low, but detectable, triacylglycerol hydrolase activity (*3*).

The aims of this study were to determine (i) if HL and EL have different substrate specificities for HDL phospholipids and (ii) and whether the interaction of EL and HL with the HDL surface is regulated by the phospholipid composition of the particles. These issues were addressed by using well-defined, homogeneous preparations of spherical rHDL that were comparable in size and contained apoA-I as the only apolipoprotein and either POPC, PLPC, PAPC, or PDPC as the sole phospholipid (*19*).

To determine if EL and HL preferentially hydrolyze different rHDL phospholipids, the kinetics of phospholipid hydrolysis in (POPC)rHDL, (PLPC)rHDL, (PAPC)rHDL, and (PDPC)rHDL that contained only CE in their core was determined. In these experiments phospholipids were the only rHDL constituents hydrolyzed by EL and HL. To determine if phospholipids regulate the interaction of EL and HL with

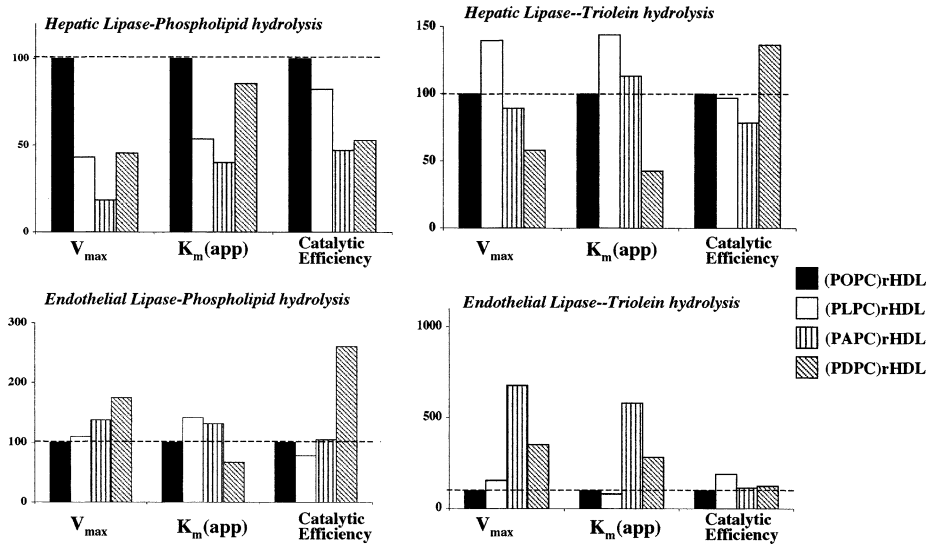

FIGURE 5: Comparison of rHDL phospholipid and TO hydrolysis by HL and EL. The V_{max}, K_m(app), and catalytic efficiency for EL- and HL-mediated phospholipid hydrolysis in (POPC)rHDL (solid bars), (PLPC)rHDL (open bars), (PAPC)rHDL (vertical bars), and (PDPC)rHDL (diagonal bars) were normalized by setting the values for (POPC)rHDL to 100. The values for the other rHDL are shown relative to (POPC)rHDL.

the rHDL surface, the kinetics of TO hydrolysis was studied in (POPC)rHDL, (PLPC)rHDL, (PAPC)rHDL, and (PDPC)rHDL that contained [^{3}H]TO in their core. In these experiments the generation of [^{3}H]NEFA from [^{3}H]TO was determined.

The results for the studies where rHDL phospholipid hydrolysis was measured showed that the V_{max} of HL-mediated phospholipid hydrolysis was higher for (POPC)rHDL than for any of the other rHDL (Figure 1A, Table 2A). This was not the case for EL, where the V_{max} of phospholipid hydrolysis was higher for the (PDPC)rHDL than for any of the other rHDL (Figure 2A, Table 2A).

These findings were unexpected because while HL and EL reportedly hydrolyze *sn*-1 acyl ester bonds (*7*, *38*), the phospholipids in the rHDL all contained palmitic acid in the *sn*-1 position and differed only in the length and unsaturation of their *sn*-2 acyl chains. There are two possible explanations for this observation. One is that the rHDL phospholipid *sn*-2 acyl chains regulate access of the *sn*-1 acyl chains to the active sites of EL and HL. This is unlikely given that during hydrolysis the *sn*-2 acyl chains are likely to partition into the rHDL surface at a location that is distant from the catalytic site of the enzyme (*39*).

The second, and more likely, possibility is that access of the phospholipid *sn*-1 acyl chains to the active sites of EL and HL is comparable for all of the rHDL and that the length and/or unsaturation of the phospholipid *sn*-2 acyl chains regulates the interaction of EL and HL with the rHDL surface. This possibility is strengthened by an earlier observation from our laboratory showing that the packing order of the phospholipid acyl chains and headgroups in spherical rHDL decreases as the unsaturation of the *sn*-2 acyl chains increases (*19*). Given that the initial interaction of HL (and presumably EL) with a substrate involves binding of the substrate to the C-terminal domain of the enzyme (*40*), it follows that changes in the properties of the substrate surface may alter this interaction.

This possibility was investigated by determining the kinetics of HL- and EL-mediated TO hydrolysis in the different types of rHDL. For these experiments increasing amounts of [^{3}H]TO-enriched rHDL were incubated with a constant amount of either EL or HL. As formation of radiolabeled NEFA was measured in these experiments, the results reflected TO, not phospholipid, hydrolysis. Moreover, as TO was the only type of triglyceride in the rHDL, it follows that variations in TO hydrolysis must reflect differences in the interaction of the enzymes with the rHDL surface. The results of these studies established that the kinetic parameters for TO hydrolysis vary according to rHDL phospholipid composition. This indicated that phospholipids do regulate the interaction of both EL and HL with the rHDL surface.

The other important finding to emerge from this study is that EL hydrolyzes triglycerides poorly compared to HL. This result, which is in agreement with what has been reported by others (*3*), may be due to the differences in the structure of the EL and HL lids. In studies of LPL, Dugi et al. established that triglyceride hydrolysis increases with increasing amphipathicity of the lid (*41*). As the residues in the HL lid are more polar than the residues in the EL lid, and the HL lid has four more positively charged residues than that of EL, it follows that the HL lid is likely to be more amphipathic than the EL lid. This could contribute to the enhanced hydrolysis of rHDL triglycerides by HL than by EL.

The fact that HL and EL have different substrate specificities for HDL phospholipids is of considerable physiological significance. Several investigators have reported that dietary fat intake can alter HDL phospholipid composition (*12*). For example, consumption of a diet high in fish and seafood enriches HDL with PDPC (*42*). According to the current results the phospholipids in these HDL will be hydrolyzed better by EL than by HL. On the other hand, a diet high in olive oil or sunflower oil, which respectively increase the POPC and PLPC content of HDL (*43*), will generate substrates that are preferred by HL. Therefore, the combined expression of both of these lipases allows for efficient hydrolysis of HDL phospholipids, regardless of dietary fat intake.

In conclusion, this study shows for the first time that HL and EL have different substrate specificities for HDL phospholipids in which the *sn*-2 acyl ester composition varies. The results also show that phospholipids affect the interaction of EL and HL with the rHDL surface. When taken together, these findings are consistent with HL and EL both contributing to optimal processing of a wide range of HDL phospholipids in vitro. If this is also found to be the case in vivo, it will establish complementary roles for both of the enzymes in HDL metabolism.

REFERENCES

1. Jaye, M., Lynch, K. J., Krawiec, J., Marchadier, D., Maugeais, C., Doan, K., South, V., Amin, D., Perrone, M., and Rader, D. J. (1999) *Nat. Genet. 21*, 424−428.
2. Hide, W. A., Chan, L., and Li, W.-H. (1992) *J. Lipid Res. 33*, 167−178.
3. McCoy, M. G., Sun, G.-S., Marchadier, D., Maugeais, C., Glick, J. M., and Rader, D. J. (2002) *J. Lipid Res. 43*, 921−929.
4. Camps, L., Reina, M., Llobera, M., Bengtsson-Olivecrona, G., Olivecrona, T., and Vilaró, S. (1991) *J. Lipid Res. 32*, 1877−1888.
5. Perret, B., Mabile, L., Martinez, L., Terce, F., Barbaras, R., and Collet, X. (2002) *J. Lipid Res. 43*, 1163−1169.
6. González-Navarro, H., Nong, Z., Freeman, L., Bensadoun, A., Peterson, K., and Santamarina-Fojo, S. (2002) *J. Lipid Res. 43*, 671−675.
7. Hirata, K-i., Dichek, H. L., Cioffi, J. A., Choi, S. Y., Leeper, N. J., Quintana, L., Kronmal, G. S., Cooper, A. D., and Quertermous, T. (1999) *J. Biol. Chem. 274*, 14170−14175.
8. Ishida, T., Choi, S., Kundu, R. K., Hirata, K.-i., Rubin, E. M., Cooper, A. D., and Quertermous, T. (2003) *J. Clin. Invest. 111*, 347−355.
9. Jin, W., Millar, J. S., Broedl, U., Glick, J. M., and Rader, D. J. (2003) *J. Clin. Invest. 111*, 357−362.
10. Homanics, G. E., de Silva, H. V., Osada, J., Zhang, S. H., Wong, H., Borensztajn, J., and Maeda, N. (1995) *J. Biol. Chem. 270*, 2974−2980.
11. Fan, J., Wang, J., Bensadoun, A., Lauer, S. J., Dand, Q., Mahley, R. W., and Taylor, J. M. (1994) *Proc. Natl. Acad. Sci. U.S.A. 91*, 8724−8728.
12. Sola, R., Motta, C., Maille, M., Bargallo, M. T., Boisnier, C., Richard, J. L., and Jacotot, B. (1993) *Arterioscler. Thromb. Vasc. Biol. 13*, 958−966.
13. Lusa, S., Jauhiainen, M., Metso, J., Somerharju, P., and Ehnholm, C. (1996) *Biochem. J. 313*, 275−282.
14. Rye, K.-A., and Duong, M. N. (2000) *J. Lipid Res. 41*, 1640−1650.
15. Davidson, W. S., Sparks, D. L., Lund-Katz, S., and Phillips, M. C. (1994) *J. Biol. Chem. 269*, 8959−8965.
16. Subbaiah, P. V., and Monshizadegan, H. (1988) *Biochim. Biophys. Acta 963*, 445−455.
17. Vézina, C. A., Milne, R. W., Weech, P. K., and Marcel, Y. L. (1988) *J. Lipid Res. 29*, 573−585.
18. Blanche, P. J., Gong, E. L., Forte, T. M., and Nichols, A. V. (1981) *Biochim. Biophys. Acta 665*, 408−419.
19. Rye, K. A., Duong, M. N., Psaltis, M. K., Curtiss, L. K., Bonnet, D. J., Stocker, R., and Barter, P. J. (2002) *Biochemistry 41*, 12538−12545.
20. Osborne, J. C., Jr. (1986) *Methods Enzymol. 128*, 213−222.
21. Rye, K.-A., and Barter, P. J. (1994) *J. Biol. Chem. 269*, 10298−10303.
22. Weisweiler, P. (1987) *Clin. Chim. Acta 169*, 249−254.
23. Rye, K.-A., Hime, N. J., and Barter, P. J. (1996) *J. Biol. Chem. 271*, 4243−4250.
24. Piran, U., and Morin, R. J. (1979) *J. Lipid Res. 20*, 1040−1043.
25. Rye, K.-A., Hime, N. J., and Barter, P. J. (1995) *J. Biol. Chem. 270*, 189−196.
26. Burstein, M., Scholnick, H. R., and Morfin, R. (1970) *J. Lipid Res. 11*, 583−595.
27. Tollefson, J. H., Lui, A., and Albers, J. J. (1988) *Am. J. Physiol. 255*, E894−E902.
28. Matz, C. E., and Jonas, A. (1982) *J. Biol. Chem. 257*, 4535−4540.
29. Martins, I. J., Lenzo, N. P., and Redgrave, T. G. (1989) *Biochim. Biophys. Acta 1005*, 217−224.
30. Hime, N. J., Barter, P. J., and Rye, K.-A. (1998) *J. Biol. Chem. 273*, 27191−27198.
31. Folch, J., Lees, M., and Stanley, G. H. S. (1957) *J. Biol. Chem. 226*, 497−509.
32. Jonas, A., Zorich, N. L., Kézdy, K. E., and Trick, W. E. (1987) *J. Biol. Chem. 262*, 3969−3974.
33. Bolin, D. J., and Jonas, A. (1994) *J. Biol. Chem. 269*, 7429−7434.
34. Takayama, M., Itoh, S., Nagasaki, T., and Tanimizu, I. (1977) *Clin. Chim. Acta 79*, 93−98.
35. Stahler, F., Gruber, W., Stinshoff, K., and Roschlau, P. (1977) *Med. Lab. 30*, 29−37.
36. Wahlefeld, A. W. (1974) in *Methods of Enzymatic Analysis*, 2nd ed., Academic Press, New York.
37. Smith, P., Krohn, R., Hermanson, G., Maillia, A., Gartner, F., Provenzano, M., Fulimoto, E., Goeke, N., Olson, B., and Klenk, D. (1985) *Anal. Biochem. 150*, 76−85.
38. Kucera, G. L., Sisson, P. J., Thomas, M. J., and Waite, M. (1988) *J. Biol. Chem. 265*, 1920−1928.
39. Carrière, F., Withers-Martinez, C., van Tilbeurgh, H., Roussel, A., Cambillau, C., and Verger, R. (1998) *Biochim. Biophys. Acta 1376*, 417−432.
40. Hill, J., Davis, R. C., Yang, D., Wen, J., Philo, J. S., Poon, P. H., Phillips, M. L., Kempner, E. S., and Wong, H. (1996) *J. Biol. Chem. 271*, 22931−22936.
41. Dugi, K. A., Dichek, H. L., Talley, G. D., Brewer, H. B., Jr., and Santamarina-Fojo, S. (1992) *J. Biol. Chem. 267*, 25086−25091.
42. Gillotte, K. L., Lund-Katz, S., de le Llera-Moya, M., Parks, J. S., Rudel, L. L., Rothblat, G. H., and Phillips, M. C. (1998) *J. Lipid Res. 39*, 2065−2075.
43. Sola, R., Baudet, M., Motta, C., Maille, M., Boisnier, C., and Jacotoc, B. (1990) *Biochim. Biopys. Acta 1043*, 43−51.

BI034990N